K^+ *LMM* resonant Auger spectra of solid KF

E. Kukk, S. Aksela, H. Aksela, E. Nõmmiste*
Department of Physics, University of Oulu, FIN-90570 Oulu, Finland

A. Kikas
Institute of Physics, Estonian Academy of Sciences, Riia 142, EE2400 Tartu, Estonia

A. Ausmees*
Department of Physics, University of Uppsala, Box 530, S-75121 Uppsala, Sweden

M. Elango
Department of Experimental Physics and Technology, Tartu University, Ülikooli 18, EE2400 Tartu, Estonia
(Received 29 April 1994)

The synchrotron-radiation-induced electron emission spectra from evaporated KF films have been measured by varying the photon energy across the K $2p$ ionization threshold. The excitation of the K $2p$ electrons to the pre-edge resonances creates resonant Auger spectra which are characterized by essentially sharper line shapes and by energy shifts of 7 eV to higher kinetic energies as compared with the normal Auger spectra.

I. INTRODUCTION

Alkali halides are ionic crystals, where the electronic structure of ions retains a great deal of the atomic character. The excitation and deexcitation spectra of these compounds show quite a strong resemblance with the spectra of isoelectronic atoms, although the influences of the solid medium can be also seen.[1,2] The comparison of the spectra, measured from atoms and ionic crystals, gives information about the solid state effects.

The K $2p^{-1}3d$ excited states in solid KF have been widely studied during the last decade.[3–7] The main features of the absorption spectrum have been explained by the spin-orbit splitting of the $2p$ orbital and by the splitting of the $3d$ orbital in the crystal field. Deexcitation of these excited states takes place mainly via the *LMM* resonant Auger transitions. The resonant Auger spectra have been studied in a number of papers during last years.[2,8,9] The measurements have been carried out using monochromatized synchrotron radiation, which allows selective resonant excitations to various excited states. The interpretation and understanding of the resonant Auger processes in potassium halides and in solids in general is far from complete, requiring additional studies. On the other hand, the resonant Auger processes in the isoelectronic argon atom ($1s^22s^22p^63s^23p^6$) have been widely studied both experimentally[10] and theoretically.[11,12] The resonant Auger spectra of Ar atom exhibit intense spectator Auger transitions, accompanied with unusually strong shake-up processes.

The synchrotron-radiation-induced electron emission spectra were measured from evaporated films of KF around the K $2p$ ionization threshold in this work. The resonant Auger spectra of potassium have been studied by carrying out detailed data handling with the aid of a curve fitting technique and by analyzing the spectra in the light of previous studies of solid potassium halides and atomic argon. The observed features of apparently nonatomic character have been tentatively interpreted on the basis of crystal field effects and the $10Dq$ theory.

II. EXPERIMENT

The measurements were performed using synchrotron radiation at MAX-lab in Lund, Sweden. The Zeiss SX-700 monochromator and Scienta SES-200 hemispherical electron energy analyzer at the beam line 22 were used.[13] The sample films were prepared *in situ* by thermal evaporation from a molybdenum boat onto polished stainless steel substrates in vacuum below 5×10^{-7} torr. The film thickness (about 100 Å) and the evaporation rate (several Å/s) were controlled by a quartz crystal monitor. The vacuum in the experimental chamber was typically 2×10^{-10} torr during the measurements.

The photon energy resolution, used in the course of measurements, was limited by the need to get good statistics in the Auger spectra in a reasonable time. For the SX-700 monochromator of beam line 22, the photon bandwidth is known to be about 0.25 eV at 300 eV photon energy with the 1221 l/mm grating and 50 μm exit slit used. The photon energy calibration was done on the basis of kinetic energy difference of the photoelectron lines created by first and the second order diffracted light. No absolute electron energy calibration was done for the spectra, but small charging effects were corrected by aligning the potassium $3p$ photolines to equal binding energies. The energy resolution of the electron spectrometer was about 0.2 eV during the recordings.

III. RESULTS

A. Absorption

The total photoabsorption cross section around the K $2p$ ionization threshold is well represented by the total electron yield spectrum, which has been recorded in the photon energy range of 296–302 eV. The spectrum displays four intense and clearly separated maxima, marked by A–D (Fig. 1). Peaks A and B correspond to the $2p_{3/2} \rightarrow 3d$ excitations. The reason for the appearance of two peaks is the crystal field splitting (CFS). The $3d$ orbital is split into two components with different orientations in the crystal field. They can be assigned to different irreducible representations of the O_h symmetry group, using the formalism of group theory.[2,6] The low-energy component (related to peak A in the absorpion spectrum) corresponds to the t_{2g} representation, whereas the high-energy component (peak B) corresponds to the e_g representation. The CFS components of the $3d$ orbital will be referred further as $3d(t_{2g})$ and $3d(e_g)$, if the distinction is essential. Peaks C and D in the absorption spectrum correspond to the $2p_{1/2} \rightarrow 3d$ transitions, similarly split by the crystal field. The low-energy shoulder at $h\nu$=296 eV may be caused by weak $2p_{3/2} \rightarrow 4s$ transitions. The energy levels of the $2p^{-1}3d$ atomic state in the crystal field have been analyzed in more detail by de Groot *et al.*[6]

According to the multiconfigurational Dirac-Fock (MCDF) calculations the $2p^{-1}3d$ excited states of the K^+ ion are close to the jj-coupling limit. The lowest-energy excitation with ΔJ=1 can thus be interpreted as the $2p_{3/2} \rightarrow 3d_{3/2}$ transitions. The energies of the $2p_{3/2} \rightarrow 3d_{5/2}$ and $2p_{1/2} \rightarrow 3d_{3/2}$ excitations are predicted to be by 1.1 eV and 3.8 eV higher, respectively. The photoexcitation probability for the $2p_{3/2} \rightarrow 3d_{3/2}$ transitions is small as compared with the $2p_{3/2} \rightarrow 3d_{5/2}$ and $2p_{1/2} \rightarrow 3d_{3/2}$ transitions. The $2p_{3/2} \rightarrow 4s$ and $2p_{3/2} \rightarrow 3d_{3/2}$ transitions are energetically degenerate and contribute to the low-energy shoulder in the absorption spectrum.

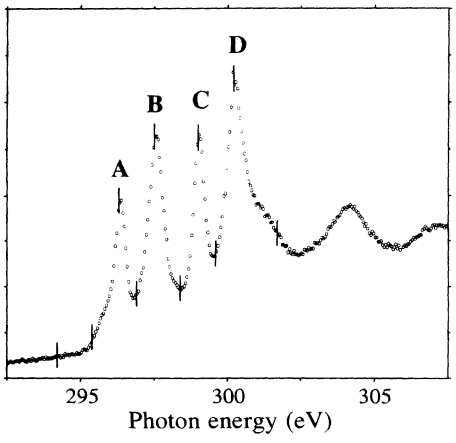

FIG. 1. Total electron yield spectrum at the K L_{23} edge. Vertical bars denote the photon energies, at which the electron spectra in Fig. 2 are recorded.

B. Deexcitation

The K LMM Auger electron spectra, recorded at the resonant photon energies around the $2p$ ionization threshold, are depicted in Fig. 2. A series of spectra has been obtained by scanning the photon energy over the absorption structures. The $L_{23}M_1M_{23}$ Auger lines appear in the kinetic energy region of 225–245 eV and the $L_{23}M_{23}M_{23}$ lines in the 240–260 eV region. The spectra contain also the K $3s, 3p$, F $2s, 2p$ photoelectron lines and the K $2p$ photoelectron line created by the second order light. The Auger electron structures and the potassium photoelectron lines display great enhancement when the energy of the exciting photons matches the absorption maxima.

The dominating structure in the resonant spectra is caused by the $L_{23}M_{23}M_{23}$ Auger transitions. In principle, the spectra consist of three groups of lines. The $2p^{-1}3d \rightarrow 3p^{-2}3d$ spectator structure appears in the spectra at resonant excitation energies, the $3d$ electron acting as a screening spectator electron during the transition. This group is shifted towards higher kinetic energies from the corresponding normal Auger lines, as seen before for Ar,[10,14] KCl,[2] and KBr.[9] The $2p^{-1}3d \rightarrow 3p^{-2}4d$ shake-up lines appear also in the spectra. The spectator Auger transitions are accompanied by the shake-up processes, because of the contraction of the spectator electron's orbital in the course of the decay process. The shake-up lines appear at lower kinetic energies than the spectator lines. The $2p^{-1} \rightarrow 3p^{-2}$ normal Auger lines appear in the resonant spectra, too, as has been seen before for potassium halides[2,9] and solid argon.[14] The reason is that the interaction with the crystal may delocalize the

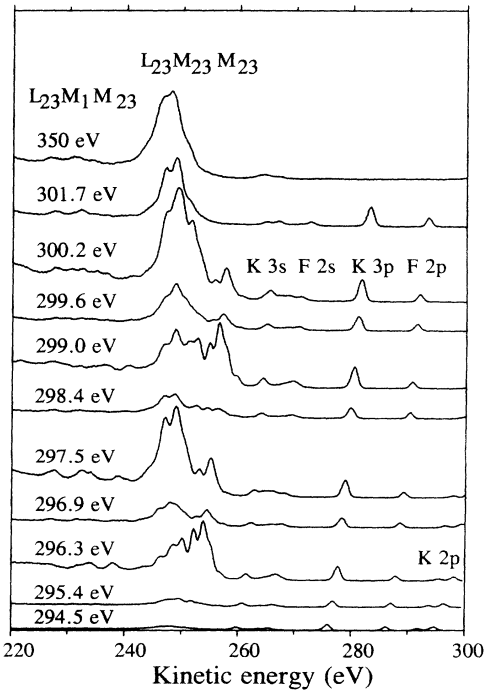

FIG. 2. A set of electron spectra of KF. The energy of excitation is marked next to each spectrum (see also Fig. 1).

$3d$ electron before the Auger decay takes place, producing $2p^{-1}$ initial states. The final state of both the L_2 and L_3 normal Auger structures consists of five components, denoted in the LS-coupling scheme by the ^1S, ^1D, and ^3P terms, the triplet term remaining unresolved. The final state of the resonant Auger transitions can be characterized by similar term structure, if the $3p-3d$ electrostatic interaction is weak with respect to the $3p-3p$ interaction.

The weak $L_{23}M_1M_{23}$ resonant Auger structure should display similar spectator, shake-up, and normal Auger features as the $L_{23}M_{23}M_{23}$ structure. The $L_{23}M_1M_{23}$ normal Auger spectrum is split into the L_2 and L_3 groups. The final state of the transitions has the ^1P and ^3P term structure.

The features of the $L_{23}M_{23}M_{23}$ resonant Auger spectra have been decomposed applying a least squares curve fitting technique. The spectra are composed of numerous strongly overlapping peaks, which is why it was essential to minimize the number of free parameters in the fits. No conclusions can be drawn on the basis of one spectrum only. The aim was to reach at a physically consistent picture through the whole series of spectra, without unexplained line shifts and changes in linewidths or intensities. Gaussian profiles and equal linewidths were used within each structure. The intensity distribution and energy splitting for the $L_3M_{23}M_{23}$ normal Auger lines in the resonant Auger spectra were taken from the L_3 component of the normal Auger spectrum recorded at $h\nu$=350 eV. The $L_2M_{23}M_{23}$ normal Auger lines were not included in the fits for the reasons explained afterwards. Line energies and intensities for the resonant Auger lines were allowed to vary freely, although the energy splitting between LS terms should not change considerably in different spectra. The variations in the energy splitting provide an estimate for the accuracy of the fits. The exception is the weak ^1S spectator Auger line, which is strongly overlapping with more intense lines and was therefore linked to the ^1D line of the same group, using corresponding data from normal Auger spectrum. This is a possible cause of a systematic error in the fits, but there was no way to determine exact values for this peak.

C. Results of decomposition

The resonant Auger spectra, decomposed with the aid of the curve fitting technique, are presented in Fig. 3. The spectra, marked by A–D, have been recorded at the photon energies of the absorption maxima A–D (Fig. 1), correspondingly. The normal Auger spectrum taken at $h\nu$= 350 eV is also included (marked by N). A background of Shirley type and a weak $L_{23}M_{23}M_{23}$ normal Auger structure, caused by the second order light from the monochromator, have been subtracted from the spectra A–D. Kinetic energies and linewidths of the Auger lines are listed in Table I. Line energies relative to the corresponding normal Auger lines at $h\nu$=350 eV are presented in Table II. Each resonant spectrum consists of three line groups with the same term structure. The $2p^{-1}3d \rightarrow 3p^{-2}3d$ spectator Auger lines appear at the highest kinetic energies and are well separated from the other structures (except the ^1S term). The ^3P lines can be resolved in this structure due to sharper line shapes and possibly slightly different intensity distribution. The spectator structure shifts towards higher kinetic energies when the photon energy is increased.

The results are less accurate for the middle shake-up structure. However, the energy splitting inside this group is rather well constant through the whole series. As can

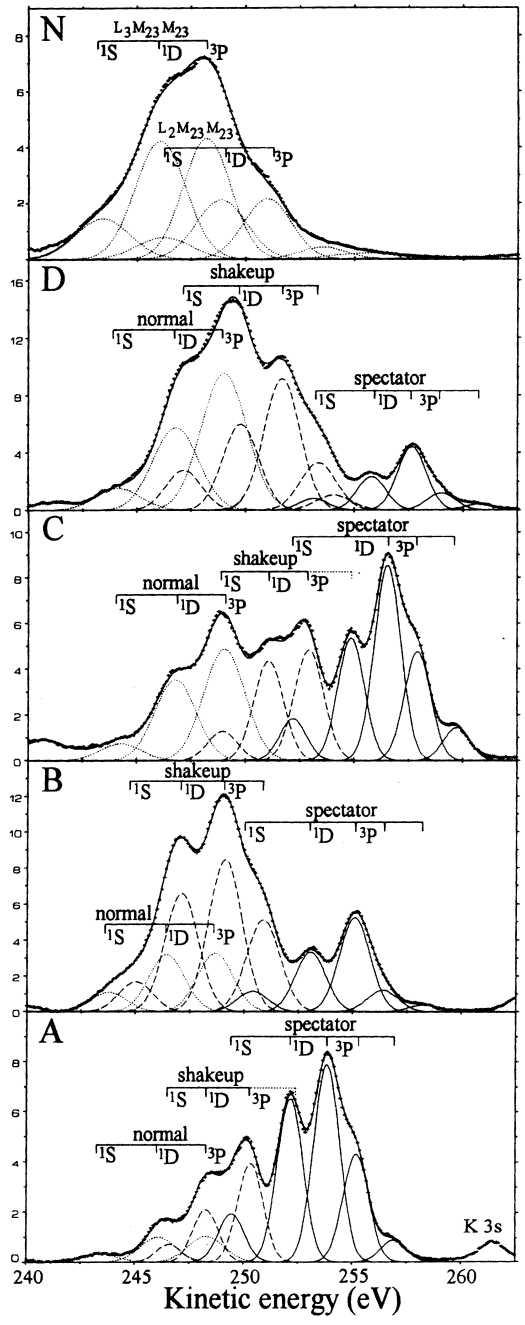

FIG. 3. Decomposed K $L_{23}M_{23}M_{23}$ resonant Auger spectra. The spectra, marked by A–D, were recorded at the photon energies matching the absorption maxima A–D of Fig. 1, correspondingly. Normal Auger spectrum (N), taken at $h\nu$=350 eV, is also included.

TABLE I. Kinetic energies and linewidths (in eV) of the ^1D resonant Auger lines and the K $3p$ photolines in the spectra, recorded at the absorption maxima A–D (spectra A–D in Fig. 3). Line energies and linewidths from the normal Auger spectrum are also included.

Spectrum		Normal Auger		Shake-up		Spectator		K $3p$	
	$h\nu$	E_k	FWHM[a]	E_k	FWHM	E_k	FWHM	E_k	FWHM
A	296.3	246.1	2.0	248.3	1.4	252.1	1.4	277.6	1.3
B	297.5	246.4	1.9	247.1	1.8	253.1	1.6	278.8	1.4
C	299.0	246.8	2.2	251.1	1.6	254.9	1.4	280.3	1.4
D	300.2	246.8	2.5	249.8	1.9	255.8	1.6	281.5	1.4
N(L_3)	350	246.0	2.7						
N(L_2)	350	248.8	2.7						

[a]Full width at half maximum (FWHM).

be seen from Table II, the energy shift of the shake-up lines with respect to the corresponding normal Auger structure is much larger if the electron shakes up from the $3d(t_{2g})$ orbital (spectra A and C) than if it shakes up from the $3d(e_g)$ orbital (spectra B and D).

The $L_3M_{23}M_{23}$ normal Auger structure in resonant spectra remains at the same kinetic energy (within error limits). The small shift toward higher kinetic energies is caused by the interaction between the Auger electron and a slow electron in the conduction band. An electron can be transferred to the conduction band either by delocalization of the electron in the $3d$ orbital or by direct photoionization. The delocalization of the $3d$ electron is the cause of the normal Auger structure only in spectra A and B, where the excited state is $2p_{3/2}^{-1}3d$. In the case of spectra C and D the photon energy is high enough to excite an electron from the $2p_{3/2}$ orbital to the conduction band, thus yielding directy the initial states of the $L_3M_{23}M_{23}$ normal Auger transitions. One could expect the appearance of the analogous $L_2M_{23}M_{23}$ normal Auger transitions in spectra C and D ($2p_{1/2}^{-1}3d$ excited state) due to the delocalization of the $3d$ electron. This structure is completely veiled by more intense lines and it is complicated to determine its intensity by the decomposition procedure. Therefore this structure is not included in the fits of spectra C and D, but its presence is manifested by somewhat disturbed intensity distribution and by widening of lines. This makes the fits of spectra C and D less accurate.

The spectrum, taken at $h\nu$=295.4 eV and shown in Fig. 2, is excited by the photons with energy matching the low-energy shoulder in the absorption spectrum. It has much lower intensity if compared to the spectra A–D in Fig. 3. The spectrum has strong contribution from the normal Auger lines, excited by the second order light from the monochromator. A weak resonant structure can be also seen, shifted by about 2 eV towards higher kinetic energies from the $L_{23}M_{23}M_{23}$ normal Auger structure. It can be assigned to the $2p_{3/2}^{-1}4s \rightarrow 3p^{-2}4s$ spectator Auger transitions.

The detailed decomposition of the $L_{23}M_1M_{23}$ resonant Auger spectra has not been carried out due to their bad statistics. The main features of the $L_{23}M_1M_{23}$ Auger transitions are revealed in Fig. 2. An extra structure appears at E_k=230–240 eV in the spectra, recorded at the photon energies matching the absorption maxima. It is composed of two peaks, separated by about 4 eV. The peaks can be assigned to the $2p^{-1}3d \rightarrow 3s^{-1}3p^{-1}3d$ spectator Auger transitions, which have retained the ^1P, ^3P final state term structure of the L_2 and L_3 normal Auger transitions. The lack of influence of the spectator electron on the term structure indicates the comparative weakness of the interaction between the $3d$ electron and the electrons involved in the decay. The displacement of the spectator lines from corresponding $L_3M_1M_{23}$ lines is about 7 eV in the spectrum, recorded at the first absorption maximum ($h\nu$=296.3 eV). The lines shift towards higher energies when the photon energy is increased. The shake-up structure is best seen in the spectrum, taken at $h\nu$=297.5 eV, where it is shifted by about 1 eV to higher energies from normal Auger lines. The normal Auger transitions contribute also to the resonant spectra. They are more pronounced in the spectra, recorded at higher photon energies (at absorption peaks C and D) than in the spectra, taken at lower photon energies.

D. Line intensities

Line intensities are determined by the decomposition procedure with rather low accuracy, giving only gen-

TABLE II. Kinetic energy shifts (in eV) of the resonant Auger lines in the spectra A–D (Fig. 3) from corresponding normal Auger lines in the spectrum N.

Spectrum	Initial state	Corresponding normal Auger	Shake-up			Spectator		
			^1S	^1D	^3P	^1S	^1D	^3P
A	$2p_{3/2}^{-1}3d(t_{2g})$	$L_3M_{23}M_{23}$	3.2	2.3	2.1	6.2	6.2	5.7
B	$2p_{3/2}^{-1}3d(e_g)$	$L_3M_{23}M_{23}$	1.7	1.2	1.0	7.1	7.1	6.9
C	$2p_{1/2}^{-1}3d(t_{2g})$	$L_2M_{23}M_{23}$	2.9	2.3	2.0	6.1	6.1	5.6
D	$2p_{1/2}^{-1}3d(e_g)$	$L_2M_{23}M_{23}$	1.1	1.0	0.7	7.0	7.0	6.7

eral trends. The total intensities of the spectator and shake-up Auger structures as a function of photon energy (Fig. 4) display strong resonance enhancements when the photon energy matches the absorption peaks A–D. The most pronounced difference between the spectra, recorded at photon energies tuned to peaks A and B, is a change in the shake-up probability. The shake-up–spectator Auger intensity ratio is $\approx$0.3 in the spectrum, corresponding to the absorption peak A, and $\approx$1.8 in the spectrum, corresponding to peak B. This branching ratio of the spectator and shake-up Auger transitions is repeated in detail in the spectra, taken at higher photon energies (peaks C and D). The shake-up probability increases in a similar way while passing to the higher resonance (peak D).

The electron in the $3d(e_g)$ orbital is less tightly bound to the potassium ion than in the $3d(t_{2g})$ orbital. It has therefore higher probability to be delocalized to prior the resonant Auger transitions, leading to normal Auger transitions instead. This explains why the intensity of the normal Auger transitions is resonating only weakly at the absorption peak A, but is resonating strongly at the peak B. A continuous increase in the intensity of the normal Auger structure is seen at higher photon energies (around peaks C and D), where the direct $2p_{3/2}^{-1}$ photoionization becomes energetically possible. The clear enhancement of the intensity, seen at peak D, is assumed to be due to the $L_2M_{23}M_{23}$ Auger transitions. These transitions, although not included in the fits, manifest themselves as an intensity increase of the $L_3M_{23}M_{23}\ ^1D$ and especially ^3P lines, which overlap with the $L_2M_{23}M_{23}$ lines. The resonant behaviour is analogous to the similar effect described at peak B.

Provided that the photon energy is high enough to excite electrons from the $2p_{1/2}$ orbital, an additional de-excitation channel may produce the $2p_{3/2}^{-1}$ states.[2] The

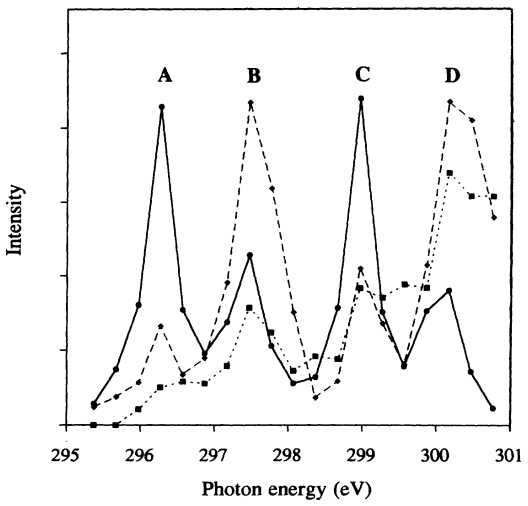

FIG. 4. Total intensity of the Auger structures in the K $L_{23}M_{23}M_{23}$ resonant Auger spectra as a function of photon energy. The intensities of the spectator, shake-up, and normal Auger structures are marked by solid, dashed, and dotted lines, respectively.

$L_2L_3M_{45}$ Coster-Kronig transitions could be energetically allowed especially in spectrum D in Fig. 3. This may reduce the intensity of the $L_2M_{23}M_{23}$ Auger transitions and enhance the intensity of the $L_3M_{23}M_{23}$ transitions, as is indeed seen in Figs. 2 and 3.

The intensities of the $L_{23}M_1M_{23}$ resonant Auger lines seem to follow the same general trends than the $L_{23}M_{23}M_{23}$ line intensities, showing resonant enhancement at the excitations matching the absorption peaks. The intensity ratios for the $L_{23}M_1M_{23}$ resonant lines cannot be studied quantitatively here due to the low intensity and high background in the spectra.

IV. DISCUSSION

A. Line shifts

The energy shifts of the resonant Auger lines could be explained by taking into account the CFS of the $3d$ and $4d$ orbitals. In a so-called $10Dq$ crystal field theory the splitting between the t_{2g} and e_g components of the d orbital is $\Delta = 10Dq$, where D describes the crystal field properties and q describes the properties of the d wave function.[5] The parameter q is determined by the quantum average of r^4 over the $3d$ or $4d$ wavefunction, as $q = 2\langle r^4\rangle_{nd}/105$. The t_{2g} and e_g states are displaced by $-4Dq$ and $6Dq$ from their unsplit energy position, respectively.

The electron in the $3d$ (or $4d$) orbital interacts rather weakly with other electrons. This assumption is supported by similar term structure and intensity distributions of the resonant and normal Auger spectra. On the other hand, the CFS is a result of the changes in the $3d$ (or $4d$) wave function in the crystal field. As a first approximation, these changes do not affect the remaining electron configuration. The initial and final state energies of Auger transitions can therefore be described by the energies of the K^+ and K^{2+} ionic state configurations (possibly affected by other solid state effects) with the CFS added as an energy correction, which depends mainly on the spatial extent of the d wave function. The larger the spatial extent, the stronger the splitting.

The electron in the $3d$ orbital remains probably in the same CFS component after the resonant Auger transition has taken place, as the d wave functions of different symmetry have different orientations and have therefore small overlap. In this case the spectator transitions are $2p^{-1}3d(t_{2g}) \rightarrow 3p^{-2}3d(t_{2g})$ in spectra A and C (Fig. 3) and $2p^{-1}3d(e_g) \rightarrow 3p^{-2}3d(e_g)$ in spectra B and D. The $3d$ orbital in the final state is more contracted due to two core holes and its splitting is smaller. The decrease of the crystal field splitting during the decay affects the energy of the outgoing Auger electron, which is higher when the spectator electron occupies the $3d(e_g)$ orbital (see Fig. 5). The energy increase is seen in Fig. 3 while passing from spectrum A to B and from C to D (see also Table II). The situation is reversed in the case of shake-up processes, where the $4d$ orbital of the Auger final state is less contracted and has larger splitting than the $3d$ or-

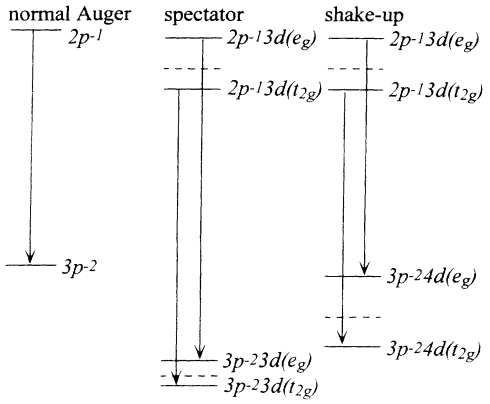

FIG. 5. Schematic energy level diagram for the K $L_{23}M_{23}M_{23}$ resonance Auger transitions.

bital of the initial state. The Auger electron has now lower energy in the $2p^{-1}3d(e_g) \rightarrow 3p^{-2}4d(e_g)$ transitions than in the $2p^{-1}3d(t_{2g}) \rightarrow 3p^{-2}4d(t_{2g})$ transitions (see Figs. 3 and 5 and Table II). The energy shifts in passing from spectrum B to C are caused by the initial state hole being in different spin-orbit split component of the $2p$ orbital.

The CFS does not play any role in the normal Auger transitions as the $3d$ orbital is unoccupied in both initial and final states and the Auger structure appears at the same kinetic energy in all spectra.

B. Shake-up processes

The results indicate that shake-up processes play an important role in the resonant Auger transitions. In the case of KBr and KCl the normal Auger structure in the resonant spectra is much stronger than in KF, because in KBr and KCl the $2p^{-1}3d$ excited states are energetically closer to the bottom of the conduction band[7] and therefore the $3d$ electron has higher probability to be delocalized prior to the Auger decay. The normal Auger decay channel is more important in KBr and KCl than in KF. The normal Auger lines dominate in KBr and KCl over the shake-up lines, which fall in the same energy region. The situation is the same also for solid argon.[14] KF seems to be most suitable among potassium halides for studying the shake-up processes.

The calculations for isoelectronic Ar atom give the probability of 0.6 for the electron in the $3d$ orbital to be shaken up during the resonant $L_{23}M_{23}M_{23}$ Auger process,[11] which agrees fairly well with experiment.[10] The calculated shake-up probability for the K^+ ion is only 0.14,[2] which is much smaller, because of the $3d$ orbital is collapsed already in the initial state. The atomic *ab initio* calculations generally overestimate the collapse of the $3d$ orbital, which manifests itself in the fact that an additional scaling of the electrostatic integrals is needed to arrive at a better agreement between experiment and theory for the final state energy splitting.[2,6,11] This indicates that the atomic calculations may not reproduce the shake-up probabilities well, either.

If the resonant Auger initial state is $2p^{-1}3d(t_{2g})$ (the lower-energy CFS component, spectra A and C in Fig. 3), then our result (shake-up probability ≈ 0.2) agrees well with calculations. In this case the $3d$ orbital points in between the ligand ions and seems to retain much of its atomic character. The shake-up probability is clearly higher (≈ 0.6) if the initial state is $2p^{-1}3d(e_g)$ (the higher-energy CFS component, spectra B and D in Fig. 3). The $3d$ orbital now points to the ligands and has larger hybridization.[6] This means a larger spatial extent of the orbital, stronger contraction during the Auger process, and higher shake-up probability. The e_g CFS component of the $3d$ orbital is strongly affected by the crystal, the effect depending also on the halide ion and lattice size. Therefore the atomic calculations are not directly applicable in this case. The hybridization of the $3d$ orbital is the strongest for KF among potassium halides.[6]

C. Auger resonant Raman effect

Near the threshold, the deexcitation following photoexcitation should basically be treated as a one-step process, the Auger resonant Raman effect,[15,16] by using a resonant scattering theory.[17,18] In the Auger resonant Raman effect, the width of the emitted resonant Auger lines reflects that of the incident radiation, not only the natural lifetime width Γ of the inner-shell hole state. If the bandwidth of the exciting radiation is narrow, then the energy of the characteristic resonant Auger line displays linear dispersion with photon energy over the range of Γ. In the experiments by Brown *et al.*[15] and by Armen *et al.*,[16] these characteristics of the Auger resonant Raman effect were confirmed for the $5d$ and $6d$ spectator Auger lines associated with the Xe $L_3M_4M_5(^1G_4)$ transitions. The $5d$ and $6d$ spectator Auger lines were found to be shifted due to screening by the spectator electron and their energies were found to exhibit linear dispersion (see Fig. 1 in Ref. 15 and Fig. 2 in Ref. 16 for details). Similar linear dispersion was also observed in a high-resolution study of Kr MNN and Xe NOO resonant Auger transitions, when the photon energy was scanned over the first resonances.[19]

In the present study of KF the $3d(t_{2g})$ and $3d(e_g)$ spectator, Auger structures have been found to peak in the spectra, recorded at the photon energies matching the absorption maxima (see Fig. 2). There is an indication of the narrowing of the spectator Auger lines (see Table I). The narrowing is due to the fact that the linewidth is determined by the bandwidth of the incident radiation and the width of the final double-hole state, if the bandwidth is narrower than the natural width of the initial state. Further measurements with varying bandwidths of the incident radiation are, however, needed at each resonance to observe the characteristics of the resonant Raman effect with clarity.

V. CONCLUSIONS

The normal, spectator, and shake-up structures have been identified in the $L_{23}M_{23}M_{23}$ Auger electron spectra

of solid KF, excited by the photons with energy near the potassium $2p$ ionization threshold. The intensity of the Auger structures is resonating strongly when the excitation energy matches the photoabsorption peaks. Resonant photoexcitation creates excited states with an electron in the previously unoccupied $3d$ orbital, which is split by the crystal field into the t_{2g} and e_g components. Distinct variations in intensity distributions and line energies have been revealed by detailed analysis of the resonant spectra, corresponding to different absorption peaks. The conclusion has been derived that the t_{2g} and e_g components of the $3d$ orbital of potassium have considerably different properties—the t_{2g} component seems to retain largely atomic character, whereas the e_g component has stronger hybridization with ligand orbitals. The dependence of the strength of splitting from the properties of the radial wave functions of the d orbitals has been roughly described using the $10Dq$ theory. An explanation for the energy shifts of the resonant Auger lines, seen in the spectra, has been proposed on the basis of different strength of crystal field splitting of the d orbitals in the Auger initial and final states.

ACKNOWLEDGMENTS

These investigations have been supported financially by the Research Council for the Natural Sciences of the Academy of Finland. The Academy of Finland and the Swedish Institute are acknowledged for providing support for A.K. and A.A., respectively. University of Oulu and the Finnish Academy of Sciences are appreciated for providing scholarships for E.K. The authors would like to thank the staff of MAX-laboratory for their assistance with the beam line 22 and the opportunity to use its experimental setup.

---

* Permanent address: Institute of Physics, Estonian Academy of Sciences, Riia 142, EE2400 Tartu, Estonia.

[1] H. Aksela, E. Kukk, S. Aksela, A. Kikas, E. Nõmmiste, A. Ausmees, and M. Elango, Phys. Rev. B **49**, 3116 (1994).
[2] M. Elango, A. Ausmees, A. Kikas, E. Nõmmiste, R. Ruus, A. Saar, J. F. van Acker, J. N. Andersen, R. Nyholm, and I. Martinson, Phys. Rev. B **47**, 11736 (1993).
[3] A. A. Maiste, R. E. Ruus, and M. A. Elango, Sov. Phys. JETP **52**, 844 (1980).
[4] M. Yanagihara, H. Maezawa, T. Sasaki, and Y. Iguchi, J. Phys. Soc. of Jpn. **54**, 3628 (1985).
[5] F. Sette, B. Sinkovic, Y. J. Ma, and C. T. Chen, Phys. Rev. B **39**, 11125 (1989).
[6] F. M. F. de Groot, J. C. Fuggle, B. T. Thole, and G. A. Sawatzky, Phys. Rev. B **41**, 928 (1990).
[7] C. Sugiura and H. Yamasaki, Jpn. J. Appl. Phys **32**, 1135 (1993).
[8] T. Tiedje, K. M. Colbow, D. Rodgers, and W. Eberhardt, Phys. Rev. Lett. **65**, 1243 (1990).
[9] A. Kikas, A. Ausmees, M. Elango, J. N. Andersen, R. Nyholm, and I. Martinson, Europhys. Lett. **15**, 683 (1991).
[10] H. Aksela, S. Aksela, H. Pulkkinen, G. M. Bancroft, and K. H. Tan, Phys. Rev. A **37**, 1798 (1988).
[11] M. Meyer, E. v. Raven, B. Sonntag, and J. E. Hansen, Phys. Rev. A **43**, 177 (1991).
[12] J. Tulkki, T. Åberg, A. Mänttykenttä, and H. Aksela, Phys. Rev. A **46**, 1357 (1992).
[13] J. N. Andersen, O. Björneholm, A. Sandell, R. Nyholm, J. Forsell, L. Thånell, A. Nilsson, and N. Mårtensson, Synch. Radiat. News **4**, 15 (1991).
[14] W. Wurth, G. Rocker, P. Feulner, R. Scheuerer, L. Zhu, and D. Menzel, Phys. Rev. B **47**, 6697 (1993).
[15] G. S. Brown, M. H. Chen, B. Crasemann, and G. E. Ice, Phys. Rev. Lett. **45**, 1937 (1980).
[16] G. B. Armen, T. Åberg, J. C. Levin, B. Crasemann, M. H. Chen, G. E. Ice, and G. S. Brown, Phys. Rev. Lett. **54**, 1142 (1985).
[17] T. Åberg, Phys. Scr. **21**, 495 (1980).
[18] T. Åberg, Phys. Scr. **T41**, 71 (1992).
[19] A. Kivimäki, A. Naves de Brito, S. Aksela, H. Aksela, O.-P. Sairanen, A. Ausmees, S. J. Osborne, L. B. Dantas, and S. Svensson, Phys. Rev. Lett. **71**, 4307 (1993).